AIChE

Process Intensification in Particle Technology: Characteristics of Powder Coatings Produced by Nonisothermal Flow-Induced Phase Inversion

Bandara Dissanayake
School of Chemical Engineering and Advanced Materials, Newcastle University, Newcastle upon Tyne NE1 7RU, UK

Andy Morgan
Akzo Nobel Powder Coatings Ltd., Stoneygate Lane, Felling, Gateshead NE10 0JY, UK

Galip Akay
School of Chemical Engineering and Advanced Materials, Newcastle University, Newcastle upon Tyne NE1 7RU, UK

DOI 10.1002/aic.12617
Published online April 27, 2011 in Wiley Online Library (wileyonlinelibrary.com).

The characteristics of powder coatings manufactured through a novel processing technique based on nonisothermal Nlow-induced phase inversion granulation enhanced by fluid injection to promote phase inversion and particle formation from melt state is summarized. Experiments were carried out in a purpose-built granulator, which operates in a parallel disk rotor-stator arrangement, so that the mechanism of granulation could be studied. The product of this intensive granulation was compared with that of the conventional powder coating manufacturing process. Understanding the mechanism of intensive granulation helped to redesign the equipment that resulted in smaller particles. Pigment dispersion characteristics were improved by intensive granulation. Also, the particle size span can be significantly reduced by dry granulation and gas-phase granulation, and the flowability can be improved by wet granulation. Chemical analysis of particles by Fourier transform infrared spectroscopic analysis showed that the injection of coolant fluid had no effect on the chemical composition. © 2011 American Institute of Chemical Engineers *AIChE J,* 58: 1060–1068, 2012
Keywords: process intensification, intensive granulation, powder coating, powder technology, flow-induced phase inversion

Introduction

Powder coating (also known as powder paint) can be considered as a green alternative to conventional solvent-based paints. The main advantage of powder coating is the absence of volatile organic compound emissions. Powder coating is currently manufactured by a comminution-based process with the following stages: (1) dry mixing; (2) melt extrusion; (3) cooling; (4) flake granulation; (5) fine grinding; (6) classification; and (7) recycling of oversized particles. Although this process is successful in industrial scale, some limitations of the process have been raised. Principally, the product of comminution-based process has a broad particle-size distribution and irregular morphology. Wide particle-size distribution

Correspondence concerning this article should be addressed to G. Akay at galip.akay@Newcastle.ac.uk.

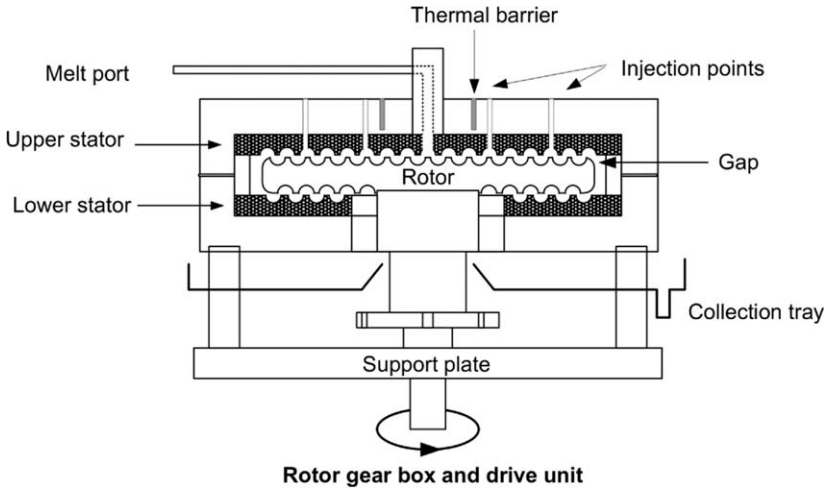

Figure 1. Schematic diagram of the intensive granulator (not to the scale).

The melt is introduced from the melt port, and the coolant (water or compressed CO_2 gas) is injected through the injection points.

and irregular particle shape cause thickness variations in powder coating films. Flow properties of the powder are very important because poorly flowing powders may cause nonuniform feed rates, deposition in spray guns, and high wastage during the application of powder coatings.[1,2] It has also been found that the dispersion of pigments in powder coating products obtained by the conventional process is poor.[3,4] Pigments should exist as primary particles rather than aggregates or agglomerates to obtain the best performance of the film. Particle clusters reduce effective scattering. Color variations can be observed when the dispersion is incomplete. The viscosity of the film is also largely influenced by the degree of pigment dispersion. The viscosity of a poor dispersion is comparatively high.[5] High viscosities retard the flow of melt during application. Poor dispersions lead to surface tension differences and consequently lead to uneven leveling. The presence of agglomerates increases the surface roughness of the film. Milling is generally energy inefficient.[6] Furthermore, the capital cost of the process is high,[7] and the process is complex involving several stages with discontinuities between them. Although the process has been improved,[8,9] in recent years, several alternative powder coating production methods have been explored to address the limitations of the conventional process.[2,10–13]

In a recent article,[14] we have developed an intensified powder coating manufacturing process based on nonisothermal flow-induced phase inversion (FIPI). Akay[15–18] discovered that FIPI and nonisothermal FIPI are fundamentally different particle generation process. In this process, a powder coating composition in molten state is phase inverted (crumbled) by a thermomechanically induced melt fracture[15–21] to produce particles by subjecting the melt to a well-defined flow field within small processing volumes. In isothermal FIPI process, the location and time of phase inversion within the equipment are dictated by the composition, thermal properties of the melt, and flow conditions. Therefore, this represented a serious problem in FIPI processes in relation to process equipment design. However, in nonisothermal FIPI,[15–17] heat-transfer conditions also play a significant role to control the location and timing of phase inversion. As heat transfer in highly viscous systems is very poor, fluid quenching has been used to circumvent poor heat transfer and control phase inversion.[14] Through this method, location of phase inversion in the processing equipment could be predetermined in FIPI processes. It was further shown that the average particle size of the product can be considerably reduced by rapid cooling, for example, by injecting a coolant/quenching fluid to the powder coating melt being processed and by carrying out phase inversion under rapid cooling and mixing.[14] In the presence of a coolant/quenching fluid, the radius at which the melt crumbles to form particles[15,20,21] was found to be weakly dependent on the processing conditions such as the powder coating to coolant ratio and coolant temperature. It was also found that because of the enhanced heat transfer, FIPI took place before the melt reached the coolant fluid injection region, thus providing a powerful method of controlling the location of crumbling. Previously reported limitations of intensive granulation (such as large crumbling radius and the average particle size of the product being equal to the rotor-stator gap[20,21]) can be eliminated[14] by using coolant injection. Water and compressed carbon dioxide (CO_2) gas were used as coolants. Intensive granulation process carried out without a coolant injection is referred to as dry granulation, whereas the process carried out with water or compressed CO_2 is referred to as wet granulation or gas-phase granulation, respectively.[14]

The main objective of this study is to characterize the product of this intensive granulation-based powder coating production process. The properties such as particle-size distribution, powder flow properties, morphology, pigment dispersion characteristics, and thermal characteristics are compared with the conventional production process. Fourier transform infrared (FTIR) spectroscopic analysis is used to validate the use of water and CO_2 in intensive granulation process.

Experimental Section

Materials

The powder coating composition is composed of a reactive binder and a filler. The specifications of the filler and the binder used in this study are given below.

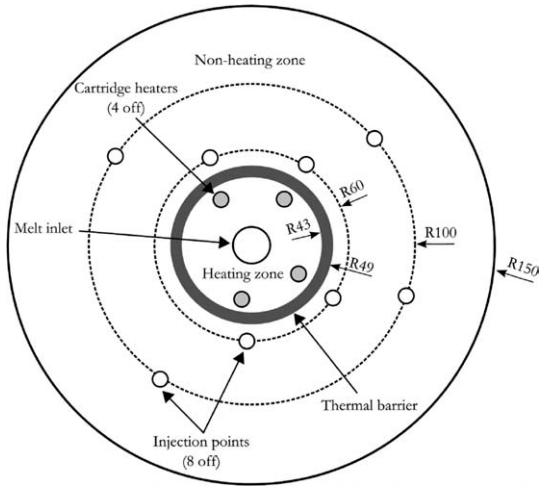

Figure 2. Diagrammatic illustration of the upper stator comprising a heating zone and a nonheating zone.

The internal diameter of injection points is 2.5 mm. Radii of various zones are indicated. All dimensions are given in millimeters.

Filler. Titanium dioxide (TiO_2) particles (coded Kronos 2310) with a mean particle size (D_{50}) of 0.2 μm was supplied by Kronos.

Binder. A carboxylic acid functional polyester (coded Polyester IP4125) with an average molecular weight of 10^4 was supplied by Nuplex Resins.

Equipments

For simplicity, the experiments are grouped into (1) intensive granulation and (2) conventional process. The equipments listed below were used in the experiments.

Extruders. Haake Rheomix 252 single-screw extruder was used for the intensive granulation experiments, and Baker Perkins MP19TC twin-screw extruder was used in the conventional process. Both extruders were laboratory extruders.

Granulator. A schematic diagram of the granulator is shown in Figure 1. It consists of a rotor block that is sandwiched between two stators. The upper stator comprises a heating zone and a nonheating zone as illustrated in Figure 2. A groove (thermal barrier) is available on the upper stator to thermally separate two zones. Heat transfer from the heating zone to the nonheating zone can effectively be reduced by running compressed air on the groove. Because the thermal barrier was not grooved completely on the upper stator, as illustrated in Figure 1, compressed air does not mix with the material being processed. Thus, compressed air injection can be considered as an indirect heat removal system.

Small circular and elongated cavities are present on the surfaces of the rotor and stators. The function[18] of the circular cavities is to mix the melt, whereas the function of elongated cavities is to pump (when melt is present) or convey (when particles are present). The melt is introduced to the granulator through an opening in the upper stator. It is subject to an angular motion due to the rotation of disks and a radial motion due to the extruder pressure. The cavities on the rotors and stators are arranged in such a way that the rotor cavities and stator cavities are offset by half a cavity length so that the melt follows a vertical path to transfer from one cavity to next cavity. As a result of the rotation, cavity arrangement, and extruder pressure, the melt flows in a three-dimensional flow path while being mixed and pumped. Details of the equipment are available elsewhere.[18,19] Another important function of these cavities is to increase the heat-transfer area to intensify heat removal from the melt. Eight injection points at two different radii are available to inject the coolant as illustrated in Figure 2.

Mill. Ultra Centrifugal Mill ZM 200 manufactured by Retsch was used to produce particles by the conventional powder coating manufacturing process. Milling stage follows the extrusion and solidification of the powder coating composition.

Experimental procedure

Intensive Granulation. A blend of carboxyl polyester (65%, w/w) and TiO_2 (35%, w/w) was prepared by dry mixing. In intensive granulation experiments, the optimum temperature profile established in our previous study[14] was used to carry out the experiments. The temperatures were as follows: (1) heating zone temperature = 70°C; and (2) nonheating zone temperature = 45°C (measured just after the thermal barrier).

The rotor–stator gap was kept at 0.5 mm in all experiments. The heating zone was first heated to 70°C, and the temperature of the nonheating zone was allowed to be established at 45°C (measured just after the thermal barrier) before the start of the experiment. The rotor speed, extruder speed, and extruder temperature were set to 30 rpm, 10 rpm, and 130°C, respectively. The rotor was heated to 30°C in dry granulation but not heated in wet granulation and gas-phase granulation. Once the temperature profile of the granulator and extruder had been established, the raw material mixture was fed to the extruder at a set rate of 10 g/min. In wet granulation experiments, water at 5°C was injected at a rate of 10 ml/min through the injection points of the upper stator. Compressed CO_2 gas at a temperature of −7°C (measured at the injection point) and pressure of 8 bar, absolute (measured at the outlet of the gas bottle) was injected in gas-phase granulation experiments. The calculated mass flow rate of CO_2 was 31 g/min. The extruder torque was constantly monitored during the run. After the completion of an experiment, the melt in the equipment was allowed to cool. Then the rotor and stator are separated for examination and evaluation of the solidified material and powder in various zones in the phase inversion process.

Conventional Process. The conventional powder coating manufacturing process was carried out using the same powder coating formula. The powder coating composition was extruded by the twin-screw extruder at a temperature of 130°C and a speed of 500 rpm. The extrudate was broken manually to obtain flakes after allowing them to cool down. They were subsequently milled using the centrifuge mill at 18,000 rpm to produce particles.

Analytical techniques

Particle-size distribution of the product was determined using a Beckman Coulter LS-230 laser diffraction particle

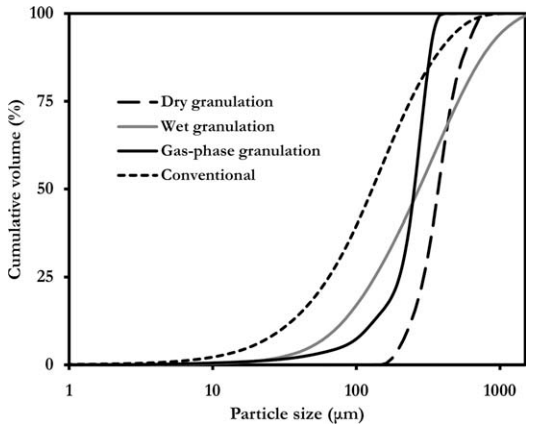

Figure 3. Particle-size distribution of the product of dry granulation, wet granulation, gas-phase granulation, and conventional process.

size analyzer. Samples were dried prior to the scanning electron microscopy (SEM), FTIR spectrometry, differential scanning calorimetry (DSC), and flowability examinations. The SEM studies were made using Philips XL30 Field Emission Gun Environmental SEM. Samples were gold coated prior to the examination. FTIR spectra of different samples were obtained using a Varian 800 FTIR spectrometer. All spectra between 600 and 4000 cm^{-1} wave number were recorded with a resolution of 2 cm^{-1}. The flowability tests were carried out using Copley JV1000 Powder Tapped Density Tester. DSC tests were performed using Mettler-Toledo FP85 DSC analyzer.

Results and Discussion

Particle size data

Particle-size distribution curves of the product of dry granulation, wet granulation, gas-phase granulation, and conventional powder coating manufacturing process are presented in Figure 3. The corresponding average particle sizes (D_{50}) and spans (S), defined in Eq. 1, are tabulated in Table 1.

$$S = \frac{D_{90} - D_{10}}{D_{50}} \tag{1}$$

where D_{10}, D_{50}, and D_{90} are the diameters below which 10, 50, and 90% of particles lie, respectively.

The particle size required for most commercial guns is up to 120 μm. When compared with intensive granulation, the conventional process produced fine particles, as can be seen from Figure 3 and Table 1. However, the particle-size distribution was very wide. The average particle size can be reduced by the injection of water or compressed CO_2 in intensive granulation. Furthermore, intensive granulation process can be characterized by the extremely narrow particle-size distribution with the exception of wet granulation. When a lump of solid material is subject to a mechanical impact, it results in few large particles and a large number of small particles. Hence, the particle-size distribution of the comminution process is generally wide.[6] It has been reported that intensive granulation process and isothermal FIPI granulation process give a narrow particle-size distribution.[18–20] It is equally applicable for dry granulation and gas-phase granulation, as can be seen from Figure 3 and Table 1. However, interestingly, the particle size span increased significantly when the product was obtained from wet granulation.

Morphology of the product

Particle Shape. SEM images of the product of dry granulation, wet granulation, gas-phase granulation, and conventional process are given in Figure 4. It further confirms that wet granulation and conventional process gave a wide particle-size distribution, whereas dry granulation and gas-phase granulation gave a narrow particle-size distribution. In addition, the product of intensive granulation appears to have approximately the same irregular morphology as the product of the conventional process.

Aspect Ratio. Shape factors are widely used to describe the shape of particles.[22–24] The aspect ratio, which is defined in Eq. 2, was obtained and the results are tabulated in Table 2.

$$\text{Aspect ratio} = L/W \tag{2}$$

where L and W are the maximum distance separating the perimeter points and the dimension of its perpendicular direction of the projection of the particle. L and W were obtained by analyzing the SEM images of the particles using GIMP software (version 2.6.3).[25]

It can be seen from the data of Table 2 that the aspect ratio of the product of intensive granulation is marginally lower than that of the product of the conventional process. A relationship between particle shape and molecular weight of the binder has been established for the isothermal FIPI granulation.[17] As the molecular weight of the binder increases, the shape of the granules deviates from the sphericity. In other words, more elongated particles are produced when high-molecular-weight binders are used. Moreover, it should be highlighted that Akay and Tong[20] also found that the morphology of the product of intensive granulation was irregular.

Because the shape of the product of intensive granulation is irregular and approximately similar to the product obtained from comminution, one might argue that the production of particles by intensive granulation process is likely to occur through comminution rather than phase inversion. However, to produce particles by comminution, the material should be subject to an adequate mechanical impact. Furthermore, the material should be at solid state, which is not the case in intensive granulation. It is very unlikely to propagate a high mechanical impact in the present granulator because the rotor speed is very low (low as 30 rpm) and the granulator operates in a parallel disk rotor–stator arrangement.

Table 1. Comparison of the Average Particle Size (D_{50}) and Particle Size Span of the Product of Dry Granulation, Wet Granulation, Gas-Phase Granulation, and Conventional Process

Method	D_{50} (μm)	Span
Dry granulation	408	0.95
Wet granulation	299	2.76
Gas-phase granulation	277	0.85
Conventional process	142	2.80

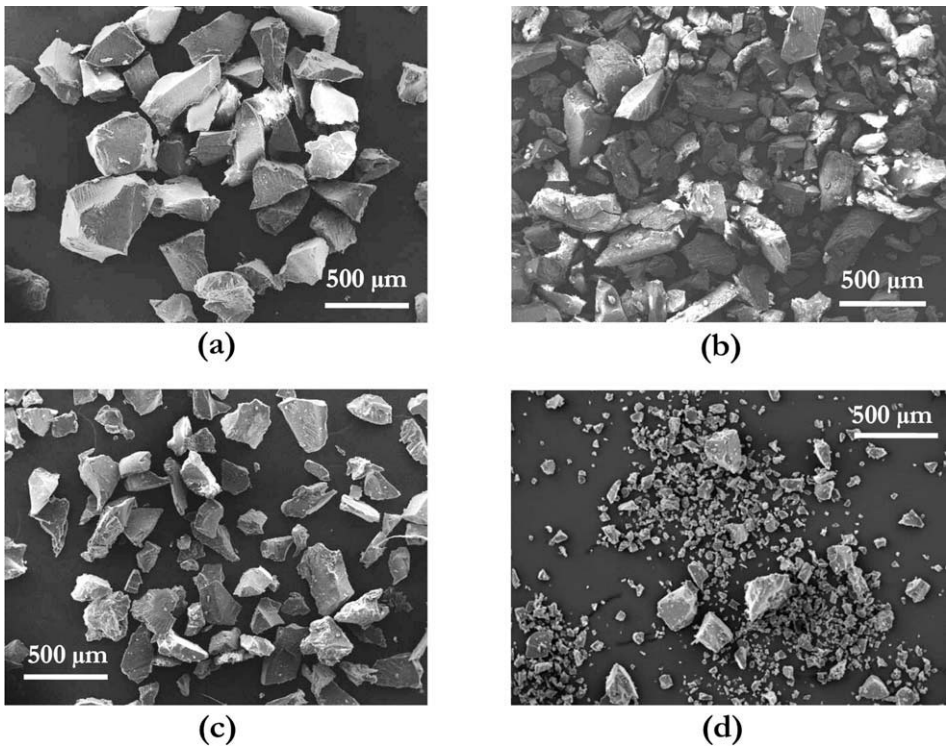

Figure 4. Comparison of the SEM images of the product of (a) dry granulation; (b) wet granulation; (c) gas-phase granulation; and (d) conventional process.

Nevertheless, Akay and Tong[21] showed that the comminution characteristic of the granulator is negligible by feeding particles through various locations of the upper stator. Furthermore, it should be pointed out that the argument of comminution leads to the formation of particles does not explain the observations made in previous studies,[14,16,20] in which it was shown that there exists four zones [(1) melt zone; (2) nucleation zone; (3) crumbling zone; and (4) granular zone] corresponding to the mechanism of the granulation. Hence, the argument that the particle formation is due to the comminution rather than the phase inversion may be ruled out.

Flowability

Compressibility of powders has been widely used in literature to describe the flowability.[26–29] Carr's compressibility index (CI) and Hausner ratio (H) defined in Eqs. 3 and 4 are used in this study to analyze powder flow properties. CI and H of the product of wet granulation and conventional process are presented in Table 3.

$$\mathrm{CI} = \frac{\rho_t - \rho_b}{\rho_t} \times 100\% \tag{3}$$

$$H = \frac{\rho_t}{\rho_b} \tag{4}$$

where ρ_t and ρ_b are the tapped density and bulk (aerated) density, respectively.

From the data of Table 3, it can be seen that the Carr's compressibility index and Hausner ratio of the product of the conventional process are higher, suggesting that the intensive granulation gave better flow properties. As the average particle size and the degree of sphericity of the product of intensive granulation are higher than that of the conventional process, better flow properties can be expected.

It can also be seen from the data of Table 3 that the bulk density and tapped density increased when particles were produced by the conventional process. The increase of the densities may be because of the presence of fine particles in the conventional product.

Differential scanning calorimetry

DSC is typically used to determine the curing reaction kinetics (curing temperature, enthalpy, and time) and storage stability (which is related to the glass transition temperature).[30–32] However, no curing agent was added to the powder coating formula because of the risk of premature reactions causing solidification of the powder coating in the extruder and equipment. Figure 5 presents the DSC heating curves of the product of dry granulation, wet granulation, gas-phase granulation, and conventional process. The

Table 2. Comparison of the Aspect Ratios of the Product of Dry Granulation, Gas-Phase Granulation, Wet Granulation, and Conventional Process

Process	Aspect Ratio
Gas-phase granulation	1.35 ± 0.23
Wet granulation	1.35 ± 0.30
Dry granulation	1.40 ± 0.33
Conventional method	1.48 ± 0.30

The quoted values are the mean aspect ratios of >50 particles with the standard deviation.

Table 3. Comparison of CI and *H* of the Product of the Conventional Process and Wet Granulation

Process	Bulk Density (kg/m^3)	Tapped Density (kg/m^3)	CI	*H*
Conventional method	798 ± 15	987 ± 22	19.1 ± 2.88	1.24 ± 0.04
Wet granulation	701 ± 11	833 ± 8	15.4 ± 2.20	1.18 ± 0.03

The quoted values of densities and indexes are the average of three samples with the standard deviation.

Table 4. Comparison of Glass Transition Temperatures of the Products of the Conventional Process, Dry Granulation, Wet Granulation, and Gas-Phase Granulation

Process	T_{go} (°C)	T_{ge} (°C)	T_{gm} (°C)
Conventional	59.3	60.1	59.7
Dry granulation	60.0	61.6	61.0
Wet granulation	62.9	63.5	63.1
Gas-phase granulation	57.2	57.9	57.5

T_{go}, T_{ge}, and T_{gm} are the onset temperature, end temperature, and midpoint temperatures, respectively.

corresponding glass transition temperatures (T_g) are presented in Table 4.

It can be seen from the curves of Figure 5, as expected, that the thermal characteristics of the product remain essentially unchanged despite the method of the production. The glass transition temperatures were approximately equal in all cases, as presented in Table 4.

Pigment dispersion

SEM images of the products can be used to qualitatively analyze the degree of pigment dispersion of the powder coatings.[3,4,33] SEM images of the products of dry granulation, wet granulation, gas-phase granulation, and conventional process are presented in Figure 6. The efficiency of pigment dispersion in the particles was quantified by counting the number of TiO_2 clusters on particle surface as observed by SEM.

It can be clearly seen from Figure 6 and Table 5 that the dispersion of pigment particles was improved by intensive granulation irrespective the processing method (i.e., with or without injecting a coolant) when compared with that of the conventional process. Particle clusters (poorly dispersed particles) can be clearly identified in Figure 6(d). There are two possible explanations for the above-observed even pigment dispersion in intensive granulation. Mixing is better in these systems when compared with the mixing in the extruder.[34]

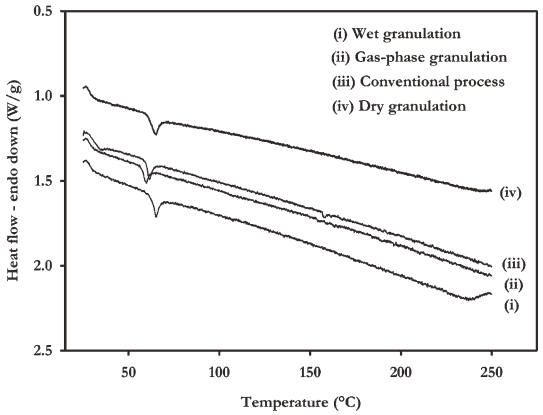

Figure 5. DSC heating curves of the products of the conventional process, dry granulation, wet granulation, and gas-phase granulation.

The heating rate was 5°C/min.

Because the melt is processed in small volumes in the cavities of the intensive granulator, it may be possible that the TiO_2 agglomerates/aggregates are deagglomerated due to the improved dispersive mixing within cavities. Another possible explanation is the steric stabilization of the pigment particles. Akay[17] reported that polymer molecules are absorbed to the surface of the particles when subject to high deformation as a stress-releasing mechanism in the isothermal FIPI granulation. The absorbed polymer layer, also known as bound polymer, forms a steric layer around pigments stabilizing the pigment dispersion. Hence, the dispersion of primary TiO_2 particles remains stable once the TiO_2 agglomerates have been deagglomerated. Steric stabilization of pigments is well established (see for example Refs. 35 and 36), and furthermore, Duivenvoorde[37] developed a block copolymer that may be used to sterically stabilize pigments in powder coating formulae.

Because the extruder used in intensive granulation was a single screw, whereas the extruder used in the conventional process was double screw, it may be argued that the comparison of the pigment dispersion characteristics in intensive granulation and conventional process is flawed. However, it is known that better pigment dispersion can be achieved using twin-screw extruder.[33] Hence, one would expect better pigment dispersion using the conventional process when compared with the intensive granulation in which a single extruder was used. Nevertheless, significant enhancement in pigment dispersion can be attributed to intensive granulation.

Fourier transform infrared spectrometry

Based on the fact that powder coating compositions generally do not react with water or CO_2, it can be expected that the injection of water or CO_2 in the granulation would not affect the chemistry of the powder coating formula. In fact, injection of water to the powder coating composition during the extrusion stage of the conventional process has been reported.[9] FTIR spectrum of the products of wet granulation and gas-phase granulation was compared with that of dry granulation to elucidate the influence of water and CO_2 on the product chemistry. The FTIR spectra are presented in Figure 7.

It is interesting to note that the absorption spectra of the products of wet granulation, dry granulation, and gas-phase granulation are apparently identical. The characteristic bands corresponding to the stretching vibration and the bending vibration of the hydroxyl group of water are generally ~3400 and ~1630 cm^{-1}, respectively.[38,39] As can be seen from Graphs (i) and (iv) in Figure 7, no peaks are observed

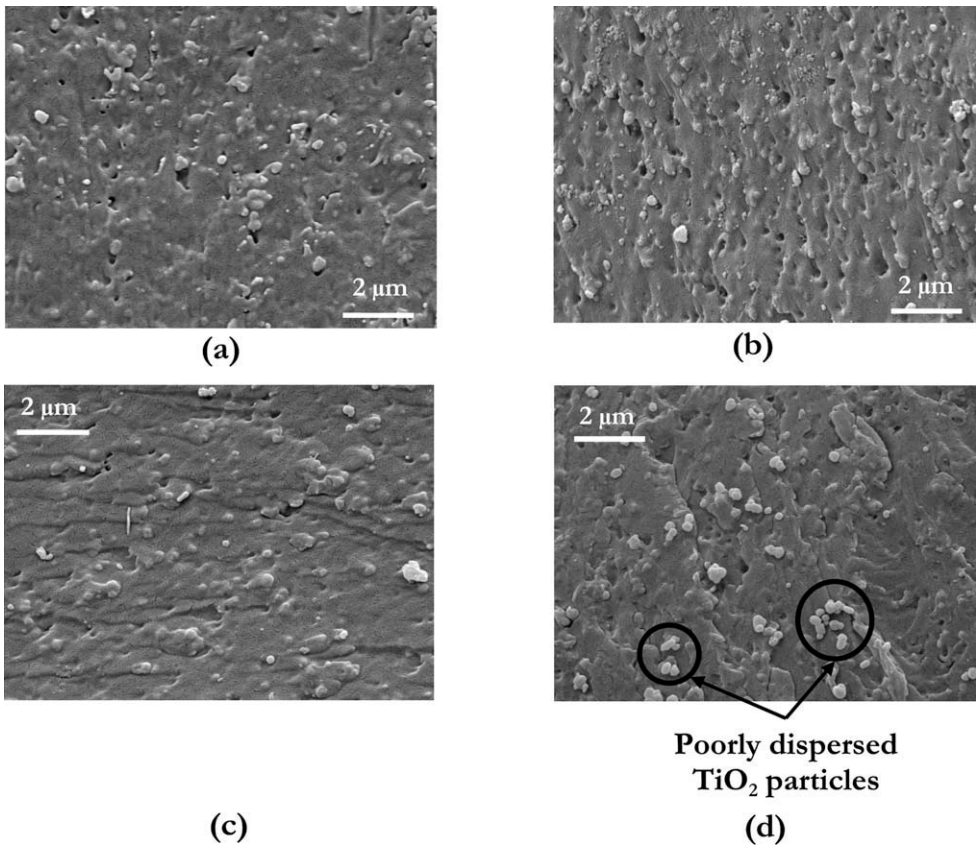

Figure 6. Dispersion of TiO_2 particles in the product of (a) dry granulation; (b) wet granulation; (c) gas-phase granulation; and (d) conventional process.

around ~3400 and ~1630 cm^{-1} in the IR spectrum of the product of wet granulation indicating that water molecules were not absorbed to the polymer or filler or encapsulated by polymer.

The peaks at ~660, ~2340, and ~1740 cm^{-1} can be assigned to the bending vibration of CO_2, stretching vibration of CO_2, and stretching vibration of the carbonyl group, respectively, to determine the interactions of CO_2 with polymers.[40,41] No peaks of the product of gas-phase granulation can be identified around ~660, ~2340, and ~1740 cm^{-1} in Graphs (ii), (iii), and (v) in Figure 7. The peak at 1716 cm^{-1} in Graph (iii) in Figure 7 may be assigned to the stretching vibration of carbonyl group (C=O) of the polymer,[42,43] whereas the peak at 1610 cm^{-1} in Graph (iv) may be assigned to aromatic ring vibration of the polymer.[44] The interaction of CO_2 with the powder coating formula during gas-phase granulation process can thus be neglected. Nevertheless, the nonexistence of any effect of CO_2 on the chemistry of the powder coating product can be understood by the fact that a carbonation reaction of the powder coatings is very unlikely to occur because CO_2 is in gaseous state and is chemically stable.

The implications of the above findings are very crucial with regards to intensive granulation process as it validates the use of water or CO_2 to reduce the average particle size of the product.

Conclusions

An alternative powder coating manufacturing process based on intensive granulation has been developed in a model granulator. Although the conventional process produced fine particles, the particle size of the product of dry granulation can significantly be reduced by injecting water (wet granulation) or compressed CO_2 (gas-phase granulation). The results of this study indicate that the pigment dispersion characteristics can be significantly improved by dry granulation, wet granulation, or gas-phase granulation when compared with the conventional process. Also, the particle size span can be significantly reduced by dry granulation and gas-phase granulation, and the flowability can be improved by wet granulation. It has been shown that the injection of water or compressed CO_2 does not

Table 5. Comparison of Number of TiO_2 Clusters in the Surface of the Product in Conventional Process, Dry Granulation, Wet Granulation, and Gas-Phase Granulation

Process	Number of Clusters per 1 m^2 Surface Area
Conventional	8.46×10^{10}
Dry granulation	3.46×10^{10}
Wet granulation	1.52×10^{10}
Gas-phase granulation	1.30×10^{10}

Number of clusters was counted from SEM images of the products.

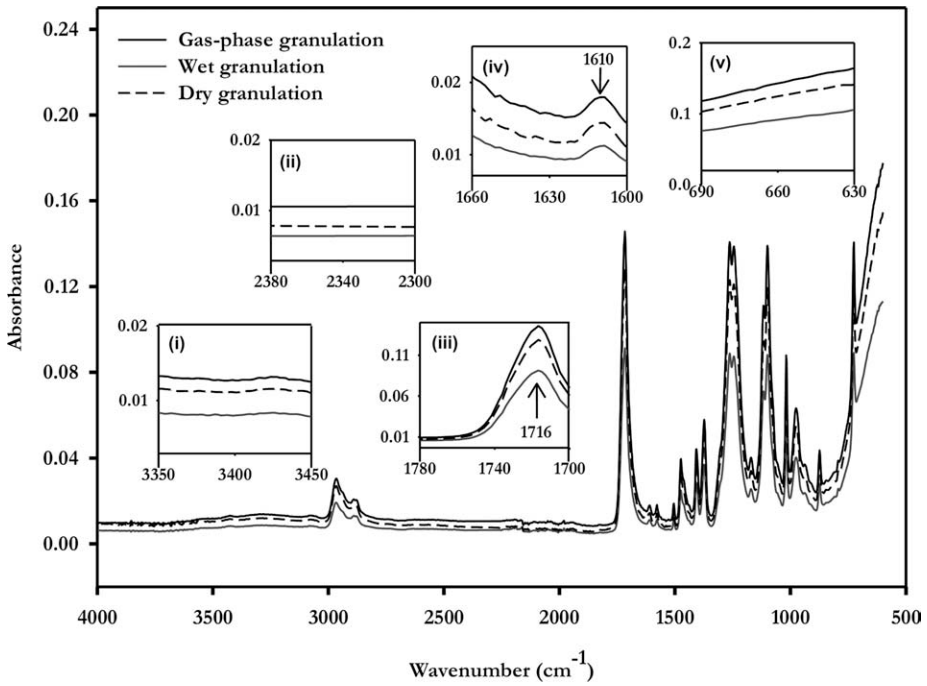

Figure 7. FTIR spectra of the product of gas-phase granulation, wet granulation, and dry granulation.

alter the chemical or thermal properties of the product. The results of this study demonstrate that this novel process has a considerable potential in the commercial scale if further developed[45] and combined with modeling.[46]

Acknowledgments

The authors thank AkzoNobel Powder Coatings, UK, for their financial support and giving permission to publish the findings. Bandara Dissanayake was supported for his PhD studies by grants from AkzoNobel and Overseas Research Students Awards Scheme jointly administrated by the UK universities. The authors also thank Dr. Paul Carter (Sunderland University) for the flowability tests.

Literature Cited

1. Daly AT, Decker OH, Wursthorn R, Houda FR, Grundowski LT, Ernst CW. Continuous processing of powder coating compositions. US Patent 6,075,074, 2000.
2. Sacripante GG, Mahabadi HK, Burns PA, Hays DA, Jugle KL. Emulsion aggregation process for forming curable powder coating compositions, curable powder coating compositions and method for using the same. European Patent EP 1,559,751, 2005.
3. Duivenvoorde FL, van Nostrum CF, van der Linde R. The pigmentation of powder coatings with the use of block copolymer dispersants. *Prog Org Coat*. 1999;36:225–230.
4. Gunde MK, Kunaver M, Mozetic M, Hrovat A. Method for the evaluation of the degree of pigment dispersion in powder coatings. *Powder Technol*. 2004;148:64–66.
5. de Lange PG. Film formation and rheology of powder coatings. *J Coat Technol*. 1984;56:23–33.
6. Richardson JF, Harker JH, Backhurst JR. *Coulson and Richardson's Chemical Engineering*, 5 ed., Vol. 2: *Particle Technology and Separation Processes*. Oxford: Butterworth-Heinemann, 2002.
7. Lee S, Lanterman HB, Pettit P, Fullerton K. Polymerisation, compatibilized blending, and particle size control of powder coatings in a supercritical fluid. PCT Publication WO 00/14145, 2000.
8. Morgan AR, Koenraadt MA, Beijers GH, Kittle KF. Process for preparing a powder coating composition. PCT Publication WO 2007/006779, 2007.
9. Morgan AR, Wilburn SR, Clark E. Powder coating extrusion process using liquid. PCT Publication WO 2009/034112, 2009.
10. Okada K, Agawa T, Shinohara K, Konishi Y. Process for producing powder coating composition, powder coating composition, and method of coating film formation. US Patent US 2003/0083402, 2003.
11. Handyside TM, Morgan AM. Powder coating compositions and process for the manufacture thereof. US Patent 5461089, 1995.
12. Adachi T, Numa N. Process for production of a powder coating. US Patent 5,763,535, 1998.
13. Ferencz JM. Bonding of powder coating compositions. US Patent US 2006/0189718, 2006.
14. Akay G, Dissanayake B, Morgan A. Process intensification in particle technology: production of powder coatings by non-isothermal flow induced phase inversion. *Ind Eng Chem Res*. In press, published on line: DOI: 10.1021/ie101516r.
15. Akay G. *Flow induced phase inversion in powder structuring by polymers*. In: Nakis N, Rosenzweig N, editors. *Polymer Powder Technology*. Chichester: Wiley, 1995:541–587.
16. Akay G. Coating process. European Patent 0,382,464, 1990.
17. Akay G. Flow induced phase inversion agglomeration: fundamentals and batch processing. *Polym Eng Sci*. 1994;34:865–880.
18. Akay G. Method and apparatus for processing flowable material and polyhipe polymers. PCT Publication WO 2004/004880, 2004.
19. Akay G, Tong L, Addleman R. Process intensification in particle technology: intensive granulation of powders by thermomechanically induced melt fracture. *Ind Eng Chem Res*. 2002;41:5436–5446.
20. Akay G, Tong L. Process intensification in particle technology: intensive granulation mechanism and granule characteristics. *J Mater Sci*. 2003;38:3169–3181.
21. Akay G, Tong L. Process intensification in particle technology: intensive agglomeration and micro-encapsulation of powders by non-isothermal FIPI. *Int J Transp Phenom*. 2003;5:227–245.
22. Blott SJ, Pye K. Particle shape: a review and new methods of characterization and classification. *Sedimentology*. 2008;55:31–63.
23. Podczeck F. A shape factor to assess the shape of particles using image analysis. *Powder Technol*. 1997;93:47–53.
24. Pons MN, Vivier H, Belaroui K, Bernard-Michel B, Cordier F, Oulhana D, Dodds JA. Particle morphology: from visualisation to measurement. *Powder Technol*. 1999;103:44–57.
25. Yekeler M, Ulusoy U, Hiçyilmaz C. Effect of particle shape and roughness of talc mineral ground by different mills on the wettability and floatability. *Powder Technol*. 2004;140:68–78.

26. Thalberg K, Lindholm D, Axelsson A. Comparison of different flowability tests for powders for inhalation. *Powder Technol*. 2004;146:206–213.
27. Liu LX, Marziano I, Bentham AC, Litster JD, White ET, Howes T. Effect of particle properties on the flowability of ibuprofen powders. *Int J Pharm*. 2008;362:109–117.
28. Wong AC. Characterisation of the flowability of glass beads by bulk densities ratio. *Chem Eng Sci*. 2000;55:3855–3859.
29. Borini GB, Andrade TC, Freitas LAP. Hot melt granulation of coarse pharmaceutical powders in a spouted bed. *Powder Technol*. 2009;189:520–527.
30. Gherlone L, Rossini T, Stula V. Powder coatings and differential scanning calorimetry: the perfect fit. *Prog Org Coat*. 1998;34:57–63.
31. Mafi R, Mirabedini SM, Attar MM, Moradian S. Cure characterization of epoxy and polyester clear powder coatings using differential scanning calorimetry (DSC) and dynamic mechanical thermal analysis (DMTA). *Prog Org Coat*. 2005;54:164–169.
32. Ramis X, Cadenato A, Morancho JM, Salla JM. Curing of a thermosetting powder coating by means of DMTA, TMA and DSC. *Polymer*. 2003;44:2067–2079.
33. Kunaver M, Gunde MK, Mozetic M, Hrovat A. The degree of dispersion of pigments in powder coatings. *Dyes Pigments*. 2003;57: 235–243.
34. Akay G, Irving GN, Kowalski AJ, Machin D. Dynamic mixing apparatus for the production of liquid composition. US Patent 6,345, 907, 2002.
35. Farrokhpay S. A review of polymeric dispersant stabilisation of titania pigment. *Adv Colloid Interface Sci*. 2009;151:24–32.
36. Tadros TF. *General principles of colloid stability and the role of surface forces*. In: Tadros TF, editor. *Colloid Stability: The Role of Surface Forces—Part 1*. Weinheim: Wiley-VCH, 2007:13–21.
37. Duivenvoorde FL. Pigment dispersing in powder coatings: synthesis and use of block copolymer dispersing agents, PhD Thesis. Eindhoven, The Netherlands: Eindhoven University of Technology, 2000.
38. Ji S, Jiang T, Xu K, Li S. FTIR study of the adsorption of water on ultradispersed diamond powder surface. *Appl Surf Sci*. 1998;133: 231–238.
39. Ichikawa K, Mori T, Kitano H, Fukuda M, Mochizuki A, Tanaka M. Fourier transform infrared study on the sorption of water to various kinds of polymer thin films. *J Polym Sci Part B: Polym Phys*. 2001;39:2175–2182.
40. Shieh Y-T, Liu K-H. The effect of carbonyl group on sorption of CO_2 in glassy polymers. *J Supercrit Fluids*. 2003;25:261–268.
41. Nalawade SP, Picchioni F, Janssen LPBM, Grijpma DW, Feijen J. Investigation of the interaction of CO_2 with poly(L-lactide), poly(DL-lactide) and poly(ε-caprolactone) using FTIR spectroscopy. *J Appl Polym Sci*. 2008;109:3376–3381.
42. Wolf MMN, Schumann C, Gross R, Domratcheva T, Diller R. Ultrafast infrared spectroscopy of riboflavin: dynamics, electronic structure, and vibrational mode analysis. *J Phys Chem B*. 2008;112: 13424–13432.
43. Klaumunzer B, Kroner D, Saalfrank P. (TD-)DFT calculation of vibrational and vibronic spectra of riboflavin in solution. *J Phys Chem B*. 2010;114:10826–10834.
44. Kiss-Eross K. *Analytical infrared spectroscopy*. In: Svehla G, editor. *Comprehensive Analytical Chemistry*, Vol. 6. Amsterdam: Elsevier Scientific Publishing, 1976:311–386.
45. Akay G, Dissanayake B. Process intensification in the production of structured granules. British Patent Application 1,018,132–9, 2010.
46. Liu L, Akay G, Tong L. Population balance modelling for a flow induced phase inversion based granulation in a two dimensional rotating agglomerator. *Chem Eng Res Des*. 2011;89:39–47.

Manuscript received Dec. 18, 2010, and revision received Feb. 18, 2011.